An Electron Tunneling Study of Superconductivity in Amorphous $Sn_{1-x}Cu_x$ Thin Films

D. G. Naugle, P. W. Watson III and K. D. D. Rathnayaka
Physics Department, Texas A&M University, College Station, TX 77843-4242

The amorphous phase of Sn would have a superconducting transition temperature near 8 K, much higher than that of crystalline Sn with $T_c = 3.5$ K. To obtain the amorphous phase, however, it is necessary to use a Sn alloy, usually Cu, and quench condense the alloy films onto a liquid He temperature substrate. Alloying with Cu reduces the superconducting transition temperature almost linearly with Cu concentration with an extrapolation of T_c to zero for $x = 0.85$. Analysis of the tunneling characteristics between a normal metal electrode with an insulating barrier and superconducting amorphous Sn-Cu films provides detailed information on the changes in the electron-phonon coupling which determines T_c in these alloys. The change from very strong electron-phonon coupling to weak-coupling with the increase in Cu content of amorphous Sn-Cu alloys for the range $0.08 \leq x \leq 0.41$ is presented and discussed in terms of theories of the electron-phonon coupling in disordered metals.

I. INTRODUCTION

It has been shown by many researchers that amorphous metals have dramatically different superconducting characteristics from their crystalline counterparts.[1-3] Knorr and Barth[4] found that the transition temperature, T_c, of an amorphous $Sn_{0.9}Cu_{0.1}$ alloy was almost 7 K, as opposed to 3.6 K for crystalline Sn. Their tunneling measurements also showed that it is a strong-coupling superconductor. Leitz[5] and Dutzi and Buckel[6] reported that the T_c of amorphous SnCu alloys decreased linearly with the Cu concentration. Heat capacity measurements of amorphous $Sn_{1-x}Cu_x$ films ($0.47 < x < 0.75$) determined that θ_D increases with increasing copper concentration.[6] The results were interpreted in terms of the McMillan[7] expression for T_c,

$$T_c = \frac{\theta_D}{1.45} \exp\left[-\frac{1.04(1+\lambda)}{\lambda - \mu^*(1+0.62\lambda)}\right] \tag{1}$$

where λ is the electron-phonon coupling constant, μ^* is the repulsive Coulomb electron-electron interaction, and θ_D is the Debye temperature. With the assumption of a constant value for μ^*, they concluded that while θ_D was increasing, evidently λ was changing in such a way as to cause a linear decrease in T_c. Dynes[8] has developed a better approximation for the transition temperature,

$$T_c = \frac{\langle\omega\rangle}{1.20} \exp\left[-\frac{1.04(1+\lambda)}{\lambda - \mu^*(1+0.62\lambda)}\right] \tag{2}$$

where $\langle\omega\rangle$ is the average phonon energy, in which $\langle\omega\rangle$ doesn't necessarily scale with θ_D. To identify the parameters responsible for the linear decrease of T_c with the copper concentration for this strong-coupling simple metal amorphous superconducting alloy, and investigate in detail the expected change from very strong-coupling to weak-coupling behavior in an amorphous metal alloy, we present tunneling measurements which have been analyzed to provide $\langle\omega\rangle$, λ, $\mu^*$and the frequency dependence of $\alpha^2F(\omega)$ for $0.08 \leq x \leq 0.41$.

II. EXPERIMENTAL DETAILS

The UHV deposition system and cryostat have been described previously[9], but the liquid-helium thermal shield has been modified to include a movable mask consisting of the horizontal and vertical slits needed to form the tunnel junctions. This allowed the entire junction to be fabricated in the UHV system and oxidation of the counterelectrode in pure O_2 at an elevated temperature instead of

in ambient room air. This *in situ* fabrication technique was essential to preparation of high quality junctions with reproducible junction resistance and low leakage characteristics.

The tunneling base electrode was made by evaporating aluminum through the horizontal slit in the liquid-helium shutter. The resulting film, 0.25 mm wide and typically 1300Å thick, was then oxidized in 1 atmosphere of dry oxygen at ~85°C for about 14 hours, resulting in a barrier oxide layer about 23Å thick. The system was then pumped overnight to a pressure of approximately 10^{-9} Torr after which the substrate was heated to ~60°C for two hours and then immediately cooled to liquid He temperature. Four SnCu films were e-beam evaporated sequentially, each deposition from an alloy ingot. The resulting films were 1 mm wide and typically 400Å thick. The base pressure before evaporation was less than 2×10^{-10} Torr with the pressure during evaporation in the mid 10^{-9} Torr range. Heating the substrate just before cooling to liquid He temperature was essential to prevent a zero-bias anomaly in the tunneling data that exhibited a $-\ln T$ dependence similar to that produced by sub-monolayers of molecular oxygen deliberately deposited on the counter electrode prior to junction formation in studies by Bermon and So.[10]

The electronics and experimental apparatus are described in more detail elsewhere.[11]

III. DATA MEASUREMENT

A. Energy Gap Determination

The input parameters to the McMillan-Rowell inversion program are the energy gap, Δ_0, and the deviation from a BCS-like superconductor. The deviation is calculated using the measured Δ_0 and the normalized tunneling density of states obtained from the raw data. Since the deviation strongly depends on Δ_0 in the low bias voltage region where the BCS density of states is changing rapidly, an incorrect determination of Δ_0 can have a large effect on the deviation. This, in turn, can cause large differences in $\alpha^2F(\omega)$ and μ^* calculated by the inversion program. Thus, an accurate determination of Δ_0 is essential in order to obtain meaningful results from the inversion program.

The determination of the energy gap is straightforward, involving the measurement of the leakage conductance and the superconducting state first derivative in the region of the gap, and was usually measured immediately after the normal state derivative. The substrate was cooled to the lowest temperature possible, ~1.5 Kelvin, while the resistance of the aluminum counterelectrode was monitored to make sure it showed no signs of superconductivity.

The leakage conductance was measured by balancing the bridge at zero bias using the smallest AC signal possible, typically less than 0.5μV. This gives $R_{\max}$, which is directly related to the leakage conductance since it should be infinite. For "good" junctions, the leakage conductance was usually less than 4% of the normal state. Zero bias was achieved by disconnecting the current sweep generator. Also, the filters were disconnected since the junction resistance was an appreciable fraction of the filters' reactance.

The superconducting state first derivative was measured with a lock-in amplifier with an AC signal typically less than 5μV and a 300 msec time constant. A very rough estimate of the gap Δ_0 was obtained by determining the voltage at which the resistance matched the high bias resistance. The bias voltage was swept starting at about $-3\Delta_0$, through zero, to about $3\Delta_0$, taking typically 20 to 30 minutes with data points about every 2μV. The sensitivity of the lock-in amplifier was set such that the lock-in didn't go off scale until the absolute value of the bias voltage was less than Δ_0. The normal and superconducting first derivative data were then smoothed and interpolated with an increment of 5μV. Data where the lock-in was off scale was not used.

The energy gap was basically determined from fitting the tunneling density of states, N_T, to the BCS density of states. This, however, is complicated by three factors: 1) the tunneling density of states is shifted slightly with respect to bias voltage due to the time constant of the lock-in amplifier; 2) the normal state first derivative data is shifted vertically from that of the superconducting state because the resistance of the film over the oxide layer is not negligible compared to the junction resistance; 3) there is a small leakage conductance. The leakage conductance is easily accounted

for by subtracting it from both the superconducting and normal state data. In terms of what is measured,

$$N_T = \frac{\sigma_S - \sigma_L}{\sigma_N - \sigma_L} = \frac{\frac{R_N}{R_S} - \frac{R_N}{R_{max}}}{1 - \frac{R_N}{R_{max}}} \tag{3}$$

where $R_N(R_S)$ is the first derivative in the normal (superconducting) state. The vertical shift in the normal state data is easily accounted for by introduction of a variable parameter, y_{offset}, and a change of variable, $R'_N = R_N + y_{\text{offset}}$.

The temperature dependent tunneling density of states in the BCS approximation is given by

$$\begin{aligned} N_T(eV,T) = \frac{dI_{sn}/dV}{dI_{nn}/dV} &= \int_{-\infty}^{\infty} dE \, \frac{N_1(E)}{N_1(0)} \frac{df(E-eV)}{dV} \\ &= \beta \int_{-\infty}^{\infty} dE \, N_{\text{BCS}}(E) \frac{e^{\beta(E-eV)}}{(1+e^{\beta(E-eV)})^2} \end{aligned} \tag{4}$$

where $N_{\text{BCS}}(E) = |E|/(E^2 - \Delta_0^2)^{1/2}$, and $\beta = (0.08617T)^{-1}$ in units of meV^{-1}. The shift in the density of states with bias voltage is accounted for by introduction of another variable parameter, x_{offset}, and a change of variable, $E' = E + x_{\text{offset}}$. The variables Δ_0, y_{offset}, and x_{offset} were varied to give the best least squares fit between equations (3) and (4). This procedure is repeated for at least three different sets of data and the resulting Δ_0's compared for consistency.

B. First Derivative Measurement

The tunneling density of states involves the measurement of the first derivatives in the normal and the superconducting states over the phonon frequency range. This is similar to the measurements needed to determine the energy gap, and in fact, the normal state first derivative had to be measured prior to actually determining the energy gap. Figure 1 is an example of the raw data for $Sn_{0.78}Cu_{0.22}$. At this stage, the AC signal was typically about $100\mu V$ so that thermal smearing was the dominant factor in the resolution of the data. Again, a 300 msec time constant on the lock-in amplifier was used, and the data was swept as slowly as possible, taking almost an hour to sweep from 0 to 50mV. Initially, data was taken with the SnCu film biased both negatively and positively. However, the junctions are not symmetric about zero bias[12], as can easily be seen in Figure 2, which is a plot of

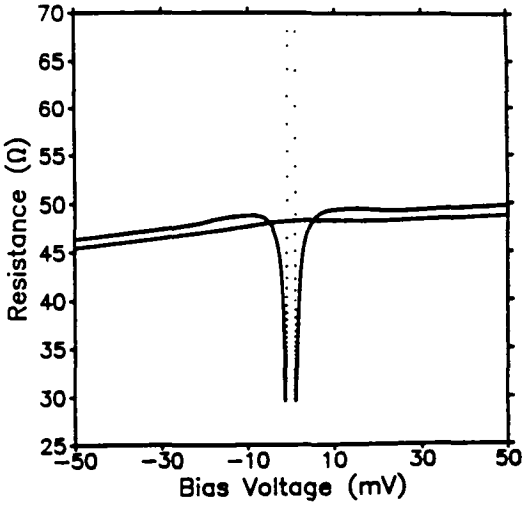

FIG. 1. Raw data for the normal state and superconducting state first derivative.

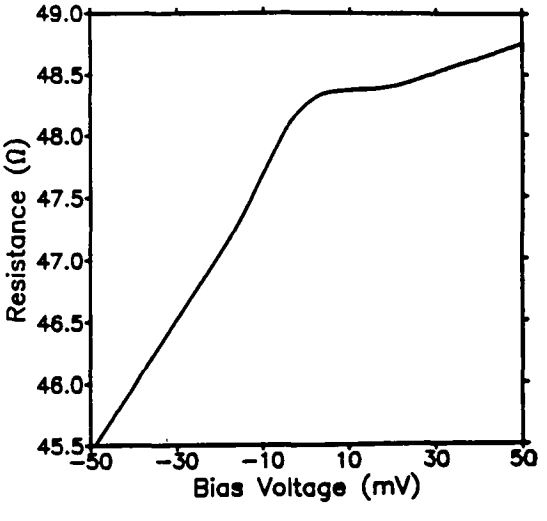

FIG. 2. The normal state first derivative raw data.

the normal state raw data. Because the junction resistance changes much more rapidly with the SnCu film biased negatively, the signal-to-noise ratio for this polarity is lower. Thus, since each polarity contained identical information, only the positively biased data was used.

The normal state first derivative was obtained by heating the substrate above the transition temperature. Since the SnCu film has a resistance in this state, this causes a small displacement of the measured first derivative above or below that measured for the superconducting state, depending on the resistivity of the film as compared to the junction resistance. Consequently, one must manually shift the data so that it matches the superconducting state at high bias voltages. Therefore, data was taken up to a bias voltage much higher than the maximum phonon energy. Thus, both the normal and superconducting state data were smoothed and interpolated with an increment of 0.05mV. The average difference was then calculated from 40mV to 50mV, and the result used to adjust the normal state data. The tunneling density of states is then given by equation (3).

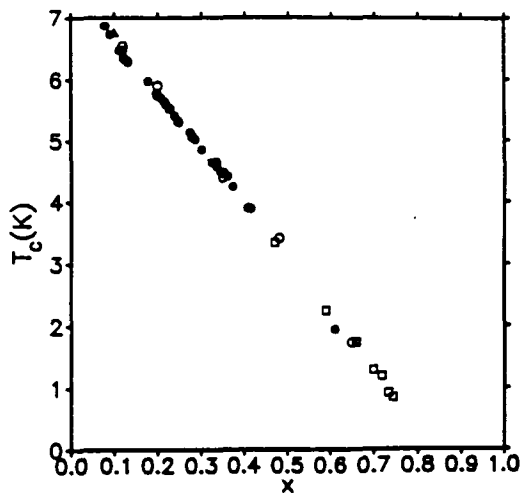

FIG. 3. Transition temperature as a function of copper concentration. The filled circles are from this study, the triangle is from Knorr and Barth[4], the open circles are from Leitz[5], and the squares are from Dutzi and Buckel[6].

IV. RESULTS AND DISCUSSION

Measurement of the superconducting transition temperature agree very well with that of others, as seen in Figure 3. Thus, the linear dependence of T_c on the copper concentration is confirmed.

Table I shows the results of the tunneling analysis, where

$$\lambda = 2\int_0^\infty \alpha^2(\omega)F(\omega)\omega^{-1}\,d\omega \tag{5}$$

$$\langle f(\omega)\rangle = \frac{2}{\lambda}\int_0^\infty \alpha^2(\omega)F(\omega)f(\omega)\omega^{-1}\,d\omega$$

$$\omega_{\log} = \exp\langle \ln\omega\rangle$$

$\omega_{\min}$ is the minimum frequency for which there is useful tunneling data. Also, the value of μ^* obtained from the inversion program is scaled to the arbitrary integration cutoff frequency ω_{co}, but $\mu^*(\omega_{ph})$ is the parameter appropriate for calculating T_c.[13] It has been rescaled to the phonon cutoff frequency ω_{ph} by

$$\frac{1}{\mu^*(\omega_{ph})} = \frac{1}{\mu^*(\omega_{co})} + \ln\left(\frac{\omega_{co}}{\omega_{ph}}\right) \tag{6}$$

Therefore, all values reported will be $\mu^*(\omega_{ph})$.

In Figure 4, $2\Delta_0/k_BT_c$ and λ are plotted as a function of copper concentration. Both $2\Delta_0/k_BT_c$ and Δ_0 decrease linearly with increasing copper concentration. Even at 41 at.% copper, the value of $2\Delta_0/k_BT_c$ is still well above the weak-coupling BCS value of 3.52. The variables in Dynes' equation for T_c are λ, μ^*, and $\langle\omega\rangle$. Values of λ determined from the tunneling measurements decrease with Cu concentration, while μ^* appears to be relatively constant (Table I) at about 0.10, which is quite different from the value of 0.04 found by Knorr and Barth[4]. $\langle\omega\rangle$ increases with increasing copper concentration, which could be expected since the average mass per atom is decreasing. Values of λ at higher Cu concentrations deduced from values of T_c and θ_D with the McMillan equation also decrease with Cu concentration,[6] but the concentration dependence is much weaker than that determined from tunneling measurements on the lower Cu concentration alloys, and there is a large discrepancy in the magnitude of λ determined in the tunneling measurements and that inferred from θ_D and T_c in the one region where the Cu concentrations are similar. This illustrates the now well known fact

TABLE I. Tunneling results. R_j is the junction resistance at 20meV. ω_{min} is the minimum energy for which there is useful tunneling data. The other quantities are defined in the text. The parameters ω_{min}, ω_{ph} and ω_{co} are given with respect to the energy gap edge, Δ_0.

Sample	SnCu#34-1	SnCu#33-4	SnCu#35-3	SnCu#35-4	SnCu#28-4	SnCu#40-3	SnCu#42-3
Concentration	$Sn_{0.92}Cu_{0.08}$	$Sn_{0.88}Cu_{0.12}$	$Sn_{0.87}Cu_{0.13}$	$Sn_{0.87}Cu_{0.13}$	$Sn_{0.78}Cu_{0.22}$	$Sn_{0.72}Cu_{0.28}$	$Sn_{0.59}Cu_{0.41}$
T_c (K)	6.865	6.332	6.302	6.283	5.585	5.068	3.905
R_j (Ω)	50	117	57	65	50	168	28
Δ_0(meV)	1.348	1.216	1.200	1.205	1.03	0.906	0.670
$2\Delta_0/k_BT_c$	4.557	4.457	4.437	4.432	4.280	4.149	3.982
Leakage (%)	1.4	1.2	0.9	0.9	4.0	4.5	4.0
ω_{min} (meV)	1.40	1.70	1.20	1.60	1.25	1.90	1.90
ω_{ph} (meV)	21	23	24	24	23	24	24
ω_{co} (meV)	110	110	110	220	110	110	110
λ	1.80	1.72	1.78	1.73	1.35	1.33	1.01
$\mu^*(\omega_{ph})$	0.089	0.114	0.118	0.116	0.079	0.113	0.090
$\langle\omega\rangle$(meV)	4.656	4.965	4.809	4.925	5.215	5.504	5.980
$\langle\omega^2\rangle^{1/2}$ (meV)	6.296	6.667	6.519	6.624	6.861	7.193	7.700
ω_{log} (meV)	2.750	2.993	2.838	2.961	3.222	3.456	3.872

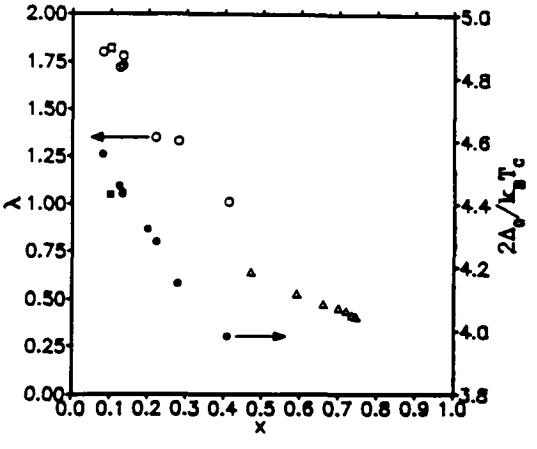

FIG. 4. λ and $2\Delta_0/k_BT_c$ as a function of copper concentration. The circles are from this study, the squares are from Knorr and Barth[4], and the triangles are values of λ from Dutzi and Buckel[6] using McMillan's T_c formula.

that the McMillan equation does not provide accurate values of λ.

Allen and Dynes[13], however, point out that equation (2) was derived with only one shape for $\alpha^2F(\omega)$. They investigated the dependence on the shape of $\alpha^2F(\omega)$ and found that the equation should be modified to be

$$T_c = \frac{f_1 f_2 \omega_{\log}}{1.20} \exp\left[-\frac{1.04(1+\lambda)}{\lambda - \mu^*(1+0.62\lambda)}\right] \quad (7)$$

where

$$f_1 = \left[1 + (\lambda/\Lambda_1)^{3/2}\right]^{1/3},$$

$$f_2 = 1 + \frac{(\overline{\omega}_2/\omega_{\log} - 1)\lambda^2}{\lambda^2 + \Lambda_2^2},$$

$$\Lambda_1 = 2.46(1 + 3.8\mu^*),$$

$$\Lambda_2 = 1.82(1 + 6.3\mu^*)(\overline{\omega}_2/\omega_{\log}),$$

$$\overline{\omega}_2 = \langle\omega^2\rangle^{1/2}$$

The functions f_1 and f_2 are fairly close to unity for the case of SnCu, so this essentially changes the prefactor to involve $\omega_{\log}$ instead of $\langle\omega\rangle$. However, $\omega_{\log}$ has a dependence on copper concentration similar to that of $\langle\omega\rangle$.

Figure 5 shows the prediction of the T_c using both equation (2) and equation (7). Neither equation gives very accurate results. Equation (2) consistently overestimates T_c by as much as 20%, whereas equation (7) consistently underestimates it. Thus, caution also should be used in routinely relying on these equations to find the microscopic parameters of a superconductor given its T_c.

Figure 6 shows plots of the $\alpha^2F(\omega)$ data found for the amorphous SnCu films in this study. As can be seen, $\alpha^2F(\omega)$ is smeared out with increasing copper concentration. There is definitely a shift to higher energies of the low energy structure, as well as an overall decrease in amplitude. The peak at ~13meV also disappears. Whether this is due to a shift to lower energies, or only to a broadening and decrease in amplitude, cannot be determined.

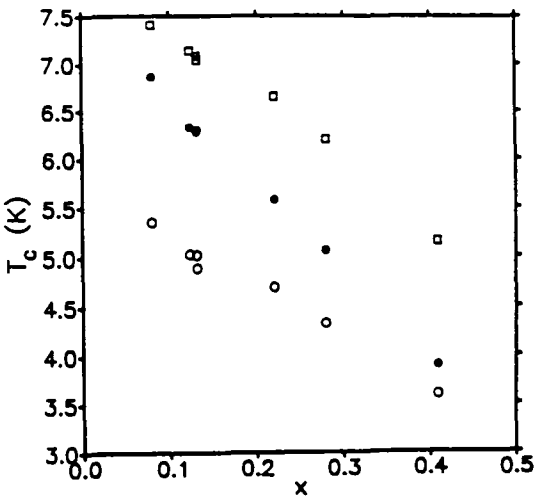

FIG. 5. Comparison between experimental and calculated values for T_c. The filled circles are experimental values from this study. The open circles are calculated using equation (7), and the open squares are calculated using equation (2).

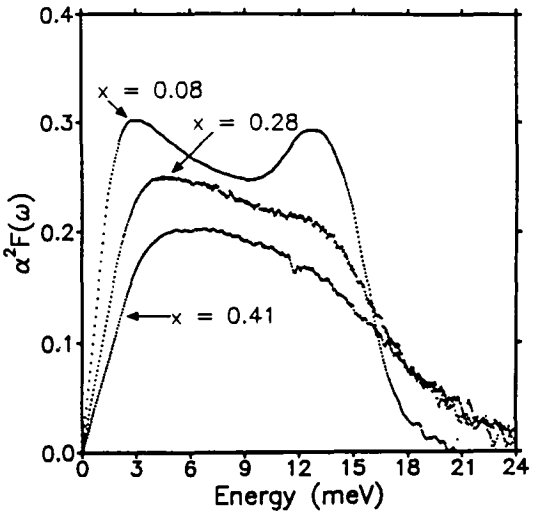

FIG. 6. $\alpha^2F(\omega)$ as a function of energy showing the data for copper concentration x = 0.08, 0.28, 0.41.

As mentioned previously there is a minimum energy, $\omega_{\min}$, above the gap edge up to which the experimental tunneling data is not useful. One cause of this is the effect of a non-zero temperature. The inversion program uses the $T = 0$ equations to obtain its results. Thus, temperature broadening, and especially taking the superconducting data at a temperature that is an appreciable fraction of the transition temperature, is not taken into account by the program. This will have the greatest effect near the gap as the data is changing rapidly there. The other major cause is the difficulty in taking data near the gap. The data was taken as a function of bias voltage by sweeping a DC current through the junction. Thus, there is a constantly changing bias voltage. This, coupled with the use of a lock-in amplifier, always results in a small offset and smearing of the data no matter how slowly the data is taken. In this respect, it would be better to use a computer-controlled voltage source that was sufficiently free of noise. Again, since the data is changing very rapidly near the gap edge, the largest effect would be seen there. Since it is not really possible to say at what point the data is good, the parameter $\omega_{\min}$ is somewhat arbitrary. Generally, it is set to the maximum energy that still gives a smooth $\alpha^2F(\omega)$ and doesn't add any extraneous structure. Again, this is somewhat arbitrary, so the additional condition that it maximizes the fit to the tunneling data was used.

Because the tunneling data is not used up to $\omega_{\min}$, a functional form for $\alpha^2F(\omega)$ must be used for this region. For most materials, this form is ω^2 and comes from the Debye theory for $F(\omega)$, assuming that $\alpha^2(\omega)$ is constant. This is usually a good approximation; however, for the SnCu films of this study, it was necessary to use $\alpha^2F(\omega) \propto \omega$ to fit the tunneling data. Knorr and Barth[4] also needed a linear dependence on ω for $\alpha^2F(\omega)$ at low energies for amorphous $Sn_{0.9}Cu_{0.1}$. Their results prompted theoretical studies for amorphous s–p superconductors[14–16] which resulted in the following theoretical expression for $\alpha^2F(\omega)$ at low frequency,

$$\alpha^2F(\omega) = \left[\frac{e^2E_F k_F^2 N(0)\rho}{3\pi^3\langle v^3\rangle mM}\right]\omega \equiv A\omega \tag{8}$$

where $N(0)$ is the electronic density of states at the Fermi energy in states/eV-atom-spin, ρ is the resistivity, M is the atomic weight, m is the electronic mass, and v is the speed of sound. The assumption of small q such that $\omega = vq$ for the phonons has been made, and

$$\frac{1}{\langle v^3 \rangle} = \frac{1}{3}\left(\frac{1}{v_l^3} + \frac{2}{v_t^3}\right)$$

where v_l and v_t are the longitudinal and transverse sound velocities, respectively. Following the approximations made by Poon and Geballe[15], the free electron model is used to obtain

$$E_F = \frac{\hbar^2 k_F^2}{2m}$$
$$N(0) = \frac{m k_F}{\pi^2 \hbar^2} \frac{M}{\rho_m A_o}$$

with ρ_m being the mass density of the alloy, and A_o is Avogadro's number. Also, $\langle v^3 \rangle \propto M\theta_D^3/\rho_m$; thus,

$$A \propto \frac{\hbar^3 k_F^5 \rho A_o}{6\pi^5 m M \theta_D^3} \tag{9}$$

Poon and Geballe[15] then determined the constant of proportionality for PbBi with known values of θ_D and $\langle v^3 \rangle$ which they assumed was the same for amorphous SnCu, 11.56. This can then be written in terms of $\langle \omega \rangle$ using McMillan's T_c equation by $\theta_D = 1.45\langle \omega \rangle / 1.20$. Thus,

$$A = \frac{11.56\hbar^3 k_F^5 \rho A_o}{6\pi^5 m M \langle \omega \rangle^3} \left(\frac{1.20}{1.45}\right)^3 \tag{10}$$

The Fermi wavevector, k_F is given by

$$k_F = \sqrt[3]{3\pi^2 \overline{Z}\, \overline{\eta}_o}$$
$$\overline{Z} = (1-x) Z_{Sn} + x\, Z_{Cu}$$

where Z_{Sn} and Z_{Cu} are the valences of the pure elements counting s- and p- states only, one for copper and four for tin. The mean number of atoms per unit volume is η_o and is given by

$$\eta_o^{-1} = (1-x)\frac{M_{Sn}}{A_o \rho_{Sn}} + x\frac{M_{Cu}}{A_o \rho_{Cu}}$$

where M_i and ρ_i are the atomic weights and the mass densities of the pure elements.

This allows calculation of the slope of $\alpha^2 F(\omega)$ to be made. Figure 7 shows a comparison between these calculations (open circles) and experimental data (closed circles) from this study. The agreement is surprisingly good considering the number of approximations made. However, this agreement is probably fortuitous, since use of values for θ_D from recent heat capacity measurements[17] in equation (9) gives very poor agreement (the open squares of Figure 7). Figure 8 shows θ_D data from the heat capacity measurements by Dutzi and Buckel[6] and Sohn[17] and $\langle \omega \rangle$ converted to θ_D using the ratios of equations (1) and (2), i.e. $\theta_D = 1.45\langle \omega \rangle / 1.20$.As seen in the figure, this commonly used relation is not valid for the amorphous SnCu system.

More fundamental than the question of what parameters to use in the calculation of A from equations (8) or (9) is the question of whether $\alpha^2 F(\omega)$ is really linear in ω at low frequency. Belitz[18] has pointed out that the derivation of equation (8) is based on incorrect assumptions and has derived the following expressions for $\alpha^2 F(\omega)$ at low frequency,

$$\alpha^2 F(\omega) = h_l^2 4k_F^3/q_D^3(\omega/E_F)\left[1 - \widehat{\rho}\frac{9}{\pi^2}\frac{4k_F}{q_D}F + O(\widehat{\rho}^2)\right], (\omega/\omega_D \ll \eta),$$

where

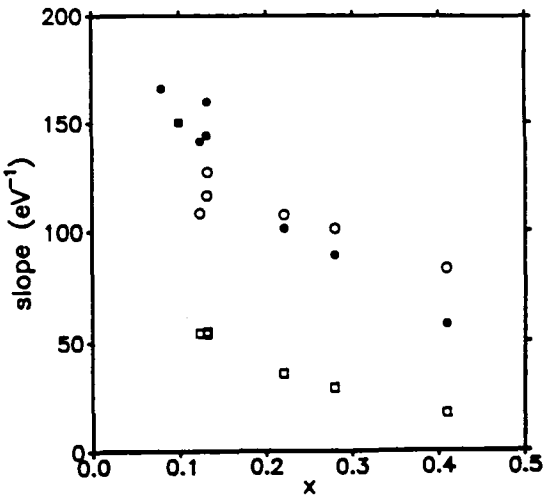

FIG. 7. Slope of $\alpha^2F(\omega)$ as a function of copper concentration. The filled circles are experimental values from this study, the filled square is from Knorr and Barth[4], the open circles are calculated values using equation (10), and the open squares are calculated values using equation (9).

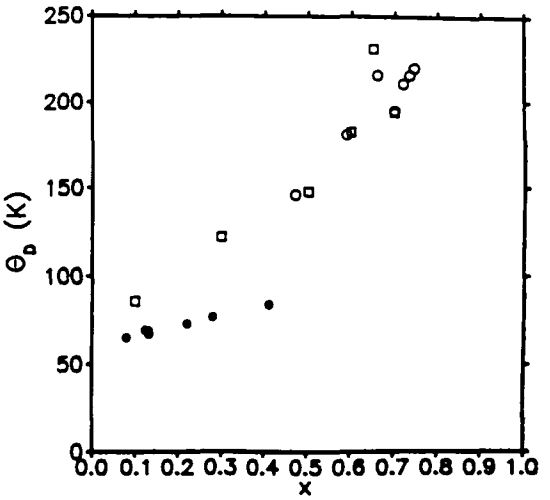

FIG. 8. θ_D as a function of copper concentration. The open circles are from Dutzi and Buckel[6], the squares are from Sohn[17], and the filled circles are from this study using $1.45\langle\omega\rangle/1.20$.

$$F = \int_0^\infty dx[\pi^2/36 - f_l^2(x)/x^2 - (v_l/v_t)^4 f_t^2(x)/x^2]$$

$$f_l(x) = \frac{1}{3}\frac{x^2 \arctan x}{x - \arctan x} - 1$$

$$f_t(x) = \frac{1}{2x^3}[2x^3 + 3x - 3(x^2+1)\arctan x];$$

$$\alpha^2F(\omega) = h_l \frac{q_D/k_F}{5\pi}\frac{8}{\widehat{\rho}}(1 + \frac{3}{2}v_l^5/v_t^5)(\omega/\omega_D)^3, \qquad (\eta \ll \omega/\omega_D \ll \widehat{\rho}\,k_F/q_D),$$

$$\alpha^2F(\omega) = h_l\left[(\omega/\omega_D)^2 + \frac{k_F/q_D}{\pi}\left[12v_l^3/v_t^3 - (8 - \pi^2/2)\right]\widehat{\rho}\,\omega/\omega_D\right], (\widehat{\rho}\,k_F/q_D \ll \omega/\omega_D \ll \widehat{\rho}\,2E_F/\omega_D)$$

where $\eta = k_F^4/9\rho_m v$, $h_l = \hbar^4 k_F^2 q_D^2 N(0)/36m^2\rho_m v_l^2$, $\widehat{\rho} = 1/k_F l$. Thus, $\alpha^2F(\omega)$ is essentially linear with ω except for the range $(\eta \ll \omega/\omega_D \ll \widehat{\rho}\,k_F/q_D)$ for which it goes as ω^3. For the SnCu films in this study, $\eta \sim 0.057$ and $\widehat{\rho}\,k_F/q_D \sim 0.080$. Thus, for $\omega_D \sim 6$meV, $\eta \sim 0.34$meV and $\widehat{\rho}\,k_F/q_D \sim 0.48$meV. Unfortunately, this range is smaller than the minimum energy for which the data of this study is reliable; so, the ω^3 region cannot be directly observed. This theory also involves v_l, v_t and θ_D which are unknown for the amorphous SnCu films of this study. An attempt was made to set $\alpha^2F(\omega)$ proportional to ω^3 up to 0.5meV and then proportional to ω up to $\omega_{\min}$ when doing the tunneling analysis. This invariably lead to an $\alpha^2F(\omega)$ and μ^* which didn't reproduce the tunneling data, as demonstrated in Figures 9 and 10 for $Sn_{0.87}Cu_{0.13}$. Figure 9 shows the resulting $\alpha^2F(\omega)$. In Figure 10 curve (a) shows the difference between the experimental tunneling density of states and the calculated density of states. There is a large difference, whereas when $\alpha^2F(\omega)$ is assumed to be proportional to ω up to $\omega_{\min}$, the difference is about 1×10^{-5}, as shown in curve (b). Also, $\mu^*(\omega_{ph})$ and λ are 0.07 and 1.46, respectively, compared with the previous results of 0.116 and

1.73. Consequently, this tunneling data is best fit by a purely linear ω dependence for $\alpha^2F(\omega)$ at low frequency in these alloys.

A material for which the range of the predicted $\alpha^2F(\omega) \propto \omega^3$ is large and at high enough energies that very accurate data can be measured would allow direct observation of the low frequency $\alpha^2F(\omega)$ spectrum to see if an ω^3 dependence exists. We are unaware of such a material. Efforts to incorporate the predicted ω^3 dependence to fit the present tunneling data were totally unsuccessful. However, it should be pointed out that Belitz's theory may be correct within the framework in which it is derived, and that this study is perhaps seeing a breakdown in the fundamental assumptions upon which this theory is based. One speculation is that perhaps the adiabatic approximation breaks down at this level of detailed measurement in such strong-coupling metals.

V. SUMMARY AND CONCLUSIONS

Amorphous $Sn_{1-x}Cu_x$ thin films ($0.08 \leq x \leq 0.41$) were prepared by e-beam deposition in an ultra-high vacuum system, forming high quality aluminum – aluminum oxide – superconductor tunnel junctions. Measurements of the transition temperature, T_c, were in excellent agreement with work done by others, confirming the linear decrease in T_c with increasing x. The superconducting energy gap, Δ_0, and $2\Delta_0/k_BT_c$ show a linear decrease with increasing x; however, $2\Delta_0/k_BT_c$ was 3.982, well above the BCS prediction of 3.52, and λ was 1.01 for $x = 0.41$, suggesting that this alloy composition is still a strong-coupling to intermediate-coupling superconductor.

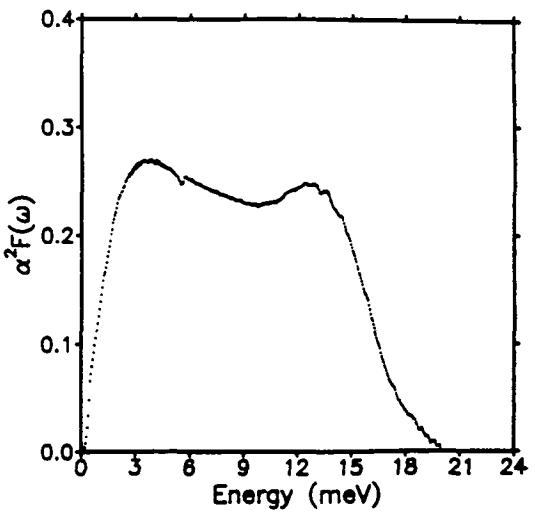

FIG. 9. $\alpha^2F(\omega)$ as a function of energy for sample SnCu#35–4 ($Sn_{0.87}Cu_{0.13}$). $\alpha^2F(\omega)$ was assumed to be proportional to ω^3 up to 0.5meV and then proportional to ω up to ω_{min}.

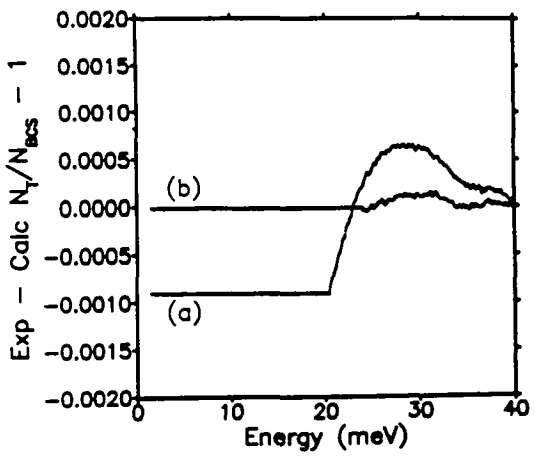

FIG. 10. Difference between the experimental and calculated tunneling density of states as a function of energy when $\alpha^2F(\omega)$ was assumed to be (a) proportional to ω^3 up to 0.5meV and then proportional to ω up to ω_{min}, and (b) linear up to ω_{min}.

The Coulomb pseudopotential is approximately independent of x, $\mu^*(\omega_{ph}) = 0.10 \pm 0.02$; λ decreases while $\langle\omega\rangle$ increases with x, indicating that λ is the cause for the decrease in transition temperature with x. The experimental values for T_c were compared to the theories of Dynes[8] and Allen and Dynes[13]. Neither formula provided quantitative agreement, suggesting that these formulae should not be routinely used to extract the microscopic parameters of a superconductor given its T_c.

A linear dependence on ω for $\alpha^2F(\omega)$ at small ω was needed to reproduce the experimental tunneling spectra in contrast to the most recent predictions which require a small region proportional

to ω^3. The shape of $\alpha^2F(\omega)$ changed from two distinct peaks at low x, to one smeared peak at $x = 0.41$. The reason for this qualitative change in the shape of $\alpha^2F(\omega)$ has not been determined.

Future work needs to be done to explore better the change from strong-coupling to weak-coupling behavior in more copper rich alloys and to better test the theories of the behavior of $\alpha^2F(\omega)$ at low frequency. This could be useful in resolving the disagreement between the theory of Belitz[18] and present data on amorphous alloys. To date there is no experimental confirmation of the detailed predictions for the low frequency behavior of $\alpha^2F(\omega)$ for strong-coupling superconductors given by this state of the art theory. A clear test will require much more accurate tunneling data near the energy gap and a strong-coupling superconductor with a broader region for the predicted ω^3 behavior.

ACKNOWLEDGMENTS

This work was supported by the Robert A. Welch Foundation, Grant No. A-0514 and the National Science Foundation, DMR-9104194. The authors acknowledge helpful discussions with D. Belitz, R. C. Dynes, G. Arnold, and E. L. Wolf. Also we thank G. Arnold for supplying a copy of the data analysis programs, and M. Sohn for providing values of his heat capacity data prior to publication.

---

[1] M. M. Collver and R. H. Hammond *Phys. Rev. Lett.* **30**, 92 (1973)
[2] G. Bergmann *Phys. Reports* **27C**, 161 (1976)
[3] W. L. Johnson and M. Tenhover, in *Glassy Metals: Magnetic, Chemical and Structural Properties*, edited by R. Hasegawa (CRC Press, Florida, 1983), p. 65.
[4] K. Knorr and N. Barth *J. Low Temp. Phys.* **4**, 469 (1971)
[5] H. Leitz *Z. Physik* B **40**, 65 (1980)
[6] J. Dutzi and W. Buckel *Z. Physik* B **55**, 99 (1984)
[7] W. L. McMillan *Phys. Rev.* **167**, 331 (1968)
[8] R. C. Dynes *Solid State Comm.* **10**, 615 (1972)
[9] D. G. Naugle, B. Bandyopadhyay, Yin Bo, V. M. Nicoli, F.-C. Wang, and D. Rathnayaka *Rev. Sci. Instrum.* **58**, 1271 (1987)
[10] S. Bermon and C. K. So *Solid State Comm.* **27**, 723 (1978)
[11] P. W. Watson III Dissertation, Texas A&M University (1993)
[12] W. F. Brinkman, R. C. Dynes and J. M. Rowell *J. of Appl. Phys.* **41**, 1915 (1970)
[13] P. B. Allen and R. C. Dynes *Phys. Rev.* B **12**, 905 (1975)
[14] G. Bergmann *Phys. Rev.* B **3**, 3797 (1971)
[15] S. J. Poon and T. H. Geballe *Phys. Rev.* B **18**, 233 (1978)
[16] L. V. Meisel and P. J. Cote *Phys. Rev.* B **23**, 5834 (1981)
[17] M. Sohn, private communication
[18] D. Belitz *Phys. Rev.* B **36**, 2513 (1987)